

1 Optimization of cleaning strategies for heliostat fields in solar tower plants

2 Giovanni Picotti^{1,2*}, Luca Moretti², Michael E. Cholette¹, Marco Binotti², Riccardo
3 Simonetti², Emanuele Martelli², Ted Steinberg¹, Giampaolo Manzolini²

4 ¹Queensland University of Technology, 2 George St, 4000, Brisbane, QLD, Australia

5 ²Dipartimento di Energia, Politecnico di Milano, via Lambruschini 4A, 20156, Milan, Italy

6

7 * Corresponding author: email g.picotti@qut.edu.au ; phone +61 07 3138 0328.

8

9 Abstract

10 The reduction due to soiling of the optical efficiency of the heliostats in the solar field is a significant detrimental factor
11 in concentrating solar power (CSP) plants. Artificial cleaning is required to maintain acceptable values of optical
12 efficiency, especially in those areas where CSP tends to be economically viable, i.e. where the yearly available DNI is
13 high and rain is scarce. The optimization of the cleaning activities is then a fundamental step to properly balance the
14 operation and maintenance (O&M) costs of the plant with the revenue losses due to soiled heliostats. In this work the best
15 cleaning schedule for a given solar field is computed through a mixed integer linear programming (MILP) model and
16 compared with the results of a heuristic approach. The optical efficiency reduction is assessed for each sector of the solar
17 field through a physical model. The MILP model accounts for the soiling impact and finds the most economical solution
18 in terms of cleaning trucks number and number of cleanings. The optimal cleaning schedule for each sector of the solar
19 field is obtained by minimizing the total cleaning cost (TCC), which is the sum of direct cleaning costs and monetized
20 losses due to soiling. A few test cases are evaluated to demonstrate the strength and the applicability of the developed
21 algorithm. The TCC improvements span between 0.7% and 19.6%, depending on the different scenarios and cost
22 structures considered. For the case studies considered, the savings due to the MILP optimized cleaning strategy were
23 between 927 kAU\$/yr and 4744 kAU\$/yr (575 k€/yr and 2941 k€/yr).

24

25 **Keywords:** Heliostat cleaning optimization; total cleaning cost minimization; solar tower plant; mixed integer linear
26 programming; operation and maintenance optimization.

27

28

29

30

31 **Nomenclature**

A_j	Area of one sector	32
A_{hel}	Heliostat area [m ²]	33
A_{soil}	Soiling area [m ²]	
C_{call}	Call cleaning cost [\$/call]	34
C_{cl}	Cleaning cost [\$/y]	
$C_{cl,fix}$	Fixed cleaning cost [\$/truck]	
$C_{cl,rent}$	Rent cleaning cost [\$/cleaning]	
$C_{cl,var}$	Variable cleaning cost [\$/cleaning]	
C_d	Airborne dust concentration [μg/m ³]	
C_{deg}	Degradation cost [\$/y]	
$C_{o\&m}$	Operation and maintenance cost (except cleaning) [\$/MWh]	
CSP	Concentrating Solar Power	
d_{cl}	Cleaning interval [days]	
DNI	Direct Normal Irradiation [kWh/m ²]	
f_{soil}	Soiling factor	
$\tilde{f}_{s,\ell,t}$	Soiling factor scheduling variable	
F_d	Flux of Dust [μg/m ² /s]	
HP	High Price	
HTF	Heat Transfer Fluid	
LCOE	Levelized Cost of Electricity [\$/MWh]	
LP	Low Price	
MILP	Mixed Integer Linear Programming	
n_{cl}	Number of cleanings	
n_{call}	Number of calls	
n_{tr}	Number of trucks	
O&M	Operation and Maintenance	
P_{el}	Electricity selling price [\$/MWh]	
PM	Particulate Matter	
PV	Photovoltaic	
Q_{rec}	Thermal power available at the receiver [MW]	
Q_{loss}	Thermal losses at the receiver [MW]	
SA	South Australia	
ST	Solar Tower	
TCC	Total Cleaning Cost [\\$]	
TP	Total Profit [\\$]	
UAE	United Arab Emirates	
v_d	Deposition velocity [m/s]	
$z_{s,\ell,t}$	Binary cleaning scheduling variable	
α_{tilt}	Tilt angle	
η_{opt}	Optical efficiency	
$\eta_{opt,clean}$	Nominal optical efficiency	
η_{pb}	Power block efficiency	
η_{th}	Receiver thermal efficiency	

35 1 Introduction

36

37 The exploitation of renewable and sustainable energy sources is one of the most important challenges the world must face
38 in the coming decades. Among the available technologies, Concentrating Solar Power (CSP) plants have the capacity to
39 provide reliable and stable power during extended periods due to the implementation of low cost thermal energy storage.
40 CSP plants harvest solar radiation through large reflecting surfaces that focus the collected power towards a receiver.
41 Among the different CSP technologies, Solar Tower (ST) plants consist of thousands of heliostats reflecting the solar
42 beams towards a central receiver, usually deployed at the top of a tall tower. The optical efficiency of the heliostats must
43 be as high as possible to maximize the solar radiation harvesting. A strongly detrimental factor that influences the optical
44 efficiency is the soiling of the heliostats, which significantly reduces their reflectance (Kutscher et al., 2010). Lower
45 optical efficiency results in lower electricity production, as the available collected power on the receiver is reduced,
46 affecting the economic profitability of the ST plant. The negative effect of heliostat soiling is primarily addressed through
47 the cleaning of the heliostats (Sarver et al., 2013). According to previous studies (Kutscher et al., 2010), the cost of
48 heliostat cleaning activities accounts for about 20% of the Operation and Maintenance (O&M) costs related to the solar
49 field, which in turn account for a 25% share of the total O&M costs for a CSP plant. Therefore, since the total O&M costs
50 (including personnel and consumables) are ~14-17% of the Levelized Cost of Electricity (IRENA and IEA-ETSAP, 2013;
51 IRENA Secreteriat et al., 2012), applying efficient cleaning strategies can potentially reduce the Levelized Cost of
52 Electricity (LCOE) by 1%, without any technology variation nor component replacement. The definition of optimal
53 cleaning strategies thus provides an important opportunity to reduce the LCOE for ST plants (Pfahl et al., 2017).

54 In literature, there are several works dealing with the optimization of the heliostat field layout (Sanchez and Romero,
55 2006), both based on energy analysis (Ortigosa et al., 2018) and techno-economic assessment (Larrayoz et al., 2019).
56 Similarly, there is large interest in the development of innovative heliostats (Pfahl et al., 2017) as well as proposing
57 different aiming strategies (Salomé et al., 2013) based on both heuristic approaches (Sánchez-González and Santana,
58 2015) and deterministic ones (Astolfi et al., 2016) to optimize the solar flux distribution on the receiver. Fewer studies
59 dealt with the specific issue of the optimal heliostat cleaning schedules, although various methods have been developed
60 (Fernández-García et al., 2014). Some studies regarding PV technologies dealt with the optimization of cleaning
61 operations: through the identification of an average soiling threshold (Fathi et al., 2017), expected power generation
62 threshold based on soiling level and environmental condition (Wang and Xu, 2018), or a rigorous mathematical
63 calculation assuming soiling production losses to vary as a decreasing exponential function (Jones et al., 2016). Other
64 studies targeting parabolic trough technologies also considered the issue of identifying the best cleaning frequency: among
65 the first, at Sandia National Laboratories, Bergeron and Freese (1981) assessed the optimal cleaning frequency based on
66 a constant soiling rate and a predicted daily direct solar energy availability. More recently, Wolferstetter et al. (2018)
67 realized a study considering a time-dependent soiling rate throughout the year to identify the most suitable cleaning
68 strategy. Although using experimental data to assess the reduced optical efficiency of the solar collectors, a homogeneous
69 soiling rate was applied on the whole solar field, and the cleaning order of the loops was always kept the same. In a follow-
70 up work, while preserving the assumption of uniform soiling rate for each solar field loop, Terhag et al. (2019) developed
71 a cleaning strategy optimization based on reinforcement learning, using an enlarged synthetic dataset of soiling rate
72 measurements collected at the Plataforma Solar de Almeria in Spain over five years.

73

74 In the authors' previous work (Picotti et al., 2019), the impact of different cleaning frequency on the average solar field
75 optical efficiency was assessed for one month of simulation, considering only direct operational cleaning costs (i.e. no
76 trucks, personnel). Depending on the chosen cleaning frequency, a fixed percentage of the solar field area was cleaned
77 each day following a pre-defined order, without investigating the impact of the chosen order.

78 Although there have been several studies on heliostat soiling and cleaning approaches, only two published papers deal
79 with the optimization of heliostat cleaning strategies. Truong Ba et al. (2017) proposed a condition-based cleaning policy
80 based on a finite Markov Decision Process which sought to minimize the total cleaning cost, i.e. the sum of revenue loss
81 due to soiling and direct cleaning costs. The proposed cleaning strategy was applied to an Australian case study and saved
82 between 5 and 30% of total cleaning costs compared with a fixed-time strategy. However, the methodology requires
83 measurement of the field-averaged reflectance and the optimization assumes that the field can be cleaned in a single day,
84 which is not realistic for large-scale CSP plants. In another study, Ashley et al. (2019) developed a cleaning procedure
85 based on a heliostat clustering and integer programming to maximize the energy collected. A heuristic method was
86 subsequently used to refine the solution to minimize the overall cleaning route length among all the clusters. The proposed
87 methodology resulted in an energy increase of 5% when compared to a simple baseline schedule. Yet, the study uses a
88 time- and space-constant soiling losses across the field and did not consider the economics, i.e. the balance of the cost of
89 cleaning activities and revenue. Thus, the provisioning of cleaning resources (e.g. trucks, personnel) was not optimized.

90 In this paper, new cleaning strategies are developed to optimize the heliostats cleaning schedule. Starting from a physical
91 model of the soiling process (Picotti et al., 2018, 2017) and measured environmental parameters (i.e. airborne dust
92 concentration, wind speed, air temperature, DNI), the (inhomogeneous) soiling losses are predicted across the solar field.
93 Based on these predictions and on the technical capabilities of the available cleaning resources, the sum of revenue loss
94 due to soiling and direct cleaning costs is minimized, identifying both the optimal provisioning of cleaning resources and
95 the optimal cleaning schedule of different sectors of the solar field.

96 With respect to previous studies, the present work has two major contributions. Firstly, the optimization is conducted
97 using soiling predictions based on a physical model that considers local conditions and inhomogeneous soiling across the
98 solar field, as opposed to the uniform or averaged efficiency losses assumed in previous studies. Secondly, the optimal
99 cleaning schedule is determined considering the economics of cleaning activities under resource limitations, which
100 enables the optimization of the cleaning resource provisioning that was neglected in earlier studies.

101 Two different strategies are developed in this study: a mixed-integer linear program (MILP) and a simplified heuristic. In
102 either case, the result of the cleaning strategy is the identification of the optimal number of sectors to be cleaned each day
103 (i.e. the number of trucks to be deployed) and the cleaning order of the different sectors. The proposed cleaning strategies
104 were numerically tested on two 100MW ST plants located in two different geographical areas with different
105 environmental conditions. The analyses are performed on yearly basis, to assess the potential of the approach and point
106 out differences in the cleaning strategies. The currency used in the economic analysis across the whole paper, unless
107 specifically indicated, is the Australian Dollar (1AUD = 0.62EUR)¹.

108 The paper is organized as follows: Section 2 presents the solar field optical efficiency model considered in the
109 optimization function focusing on the sectorial division and the soiling rate assessment. Section 3 discusses the heuristic
110 and deterministic optimization approaches adopted. Section 4 describes the case studies selected for the analysis and
111 results are reported and analysed in Section 5. Finally, the last section draws some general conclusions on the different
112 approaches pointing out some possibilities for future studies.

113 2 Sectorial optical efficiency assessment

114

115 The cleaning strategy optimization requires the evaluation of the optical efficiency of the different heliostats, depending
 116 on their relative position in the solar field. The optical efficiency is computed as the product of two main terms: the optical
 117 efficiency of clean heliostats $\eta_{opt, clean}$ and the soiling factor f_{soil} . It must be stressed that both terms are time-dependant
 118 and change for each heliostat, depending on its relative position and tracking motion. Therefore, both the optical efficiency
 119 in clean conditions and the soiling factor must be computed on a relatively short time basis (hourly in this work) for the
 120 entire year so that:

$$\eta_{opt_h} = \eta_{opt, clean_h} \cdot f_{soil_h} \quad (1)$$

121 To reduce the computational time required for the assessment of the optical efficiency of each heliostat, the solar field is
 122 divided into sectors with an equal number of heliostats. Each sector is characterized by a representative heliostat that is
 123 located in its geometrical barycentre. The number of sectors depends on the solar field size and cleaning speed in terms
 124 of square meters of heliostats per hour, which eventually determines the number of angular and radial partitions of the
 125 solar field. Further considerations could be required if also considering the computational time and capacity. The soiling
 126 model used in this work to compute the soiling factor was discussed in previous publications (Picotti et al., 2019, 2018)
 127 and only the main outcomes of these studies are described in this paper for brevity.

128 The amount F_d of dust that falls on the heliostats is calculated from the airborne dust concentration C_d , which is considered
 129 uniform over the entire solar field, the deposition velocity v_d , and the tilt angle α_{tilt} as (Picotti et al., 2019, 2018):

$$F_d = C_d \cdot v_d \cdot \cos(\alpha_{tilt}) \quad (2)$$

130 The tilt angle must be computed for each time step since it depends on both the position of the heliostat around the solar
 131 field and on the tracking movement. Moreover, it also influences the shading and blocking impact of the particles: the
 132 two effects are considered together to evaluate the area of the heliostat A_{soil} whose reflection is hindered by the soiling.
 133 A soiling factor representative of soiling-related optical losses is then determined as:

$$f_{soil} = \left(1 - \frac{A_{soil}}{A_{hel}}\right) \quad (3)$$

134 where A_{hel} is the total surface area of each heliostat. The hourly soiling factor is computed for each sectorial division of
 135 the solar field.

136 The computed optical and optical ‘as-clean’ efficiencies are then weighted by the DNI to obtain daily values as:

$$DNI_{day} = \sum_1^{24} DNI_h \quad (4)$$

$$\eta_{opt, clean}^{day} = \frac{\sum_1^{24} \eta_{opt, clean_h} \cdot DNI_h}{\sum_1^{24} DNI_h} \quad (5)$$

$$\eta_{opt}^{day} = \frac{\sum_1^{24} \eta_{opt_h} \cdot DNI_h}{\sum_1^{24} DNI_h} \quad (6)$$

137 The daily soiling factor f_{soil}^{day} , which represents the impact of soiling, is then calculated as the ratio between the optical
 138 efficiency and the optical ‘as clean’ efficiency on a daily basis:

$$f_{soil}^{day} = \frac{\eta_{opt}^{day}}{\eta_{opt, clean}^{day}} \quad (7)$$

139 The rigorous prediction of the optical efficiency losses due to soiling for each sector represents an extremely valuable
 140 input for the optimization of the solar field cleaning strategy, according to the methodology described in the next section.

141

142 3 Optimization methodology

143

144 An efficient cleaning strategy definition must ultimately aim at maximizing the plant revenues (and thus the profit),
 145 defining the number of trucks to be purchased/hired to perform cleaning activities and the cleaning schedule for each
 146 solar field sector based on the trade-off between plant productivity increases and cleaning O&M costs. The resulting
 147 optimization problem can be stated as follows. Given:

- 148 - yearly profiles of incremental heliostat soiling factor for each solar field sector (provided by the model detailed
 149 in Section 2);
- 150 - yearly profiles of solar irradiance and heliostat optical ‘as-clean’ efficiencies;
- 151 - receiver thermal losses and power block conversion efficiencies;
- 152 - variable and fixed costs related to hiring and dispatching each cleaning crew;
- 153 - electricity selling prices;

154 determine:

- 155 - the required number of cleaning crews;
- 156 - the cleaning schedule of each solar field sector (i.e. the days throughout the year in which the sector is cleaned).

157 The optimal cleaning schedule must account for limitations on cleaning crew working hours per shift. For the sake of
 158 simplicity (but without loss of generality), the sectorial size is determined so that one crew composed of 4 operators who
 159 operate a single truck can clean one sector in one day (12 working hours) and that all the aforementioned profiles are
 160 sampled with a time-step equal to one day. The optimization aims at maximizing the yearly plant revenue, or equivalently
 161 at minimizing the sum of yearly cleaning O&M cost and costs related to lost energy production with respect to the ideal
 162 perfectly clean solar field.

163 In all the computations performed in this study, it is assumed that (i) a cleaning event restores the reflectance of the
 164 heliostats to their nominal value, so that $f_{soil} = 1$, hence $\eta_{opt} = \eta_{opt, clean}$ and (ii) the soiling evolution is not modified
 165 by the cleaning operations (i.e. each daily variation of soiling factor Δf_{soil} is not dependent on the current value of f_{soil}).
 166 Thus, combining 1) the assessment of the soiling factor and optical efficiency performed in Section 2, 2) the definition of
 167 a cleaning schedule for each of the N_s sectors, and 3) the assumption that the SF solar multiple and the storage are large
 168 enough to avoid defocusing and guarantee a continuous operation, the thermal energy available at the receiver can be
 169 calculated as:

$$Q_{rec}^{day} = DNI_{day} \cdot \sum_{j=1}^{N_s} A_j \cdot \eta_{opt, clean, j}^{day} \cdot f_{soil, j}^{day} \quad (8)$$

170 Once the thermal energy available at the receiver has been determined, it is possible to evaluate the expected electricity
 171 generation considering the thermal receiver efficiency (η_{th}) and the power block efficiency (η_{pb}). The daily thermal

172 receiver efficiency is computed considering constant heat losses equal to 15% of the design thermal power available at
 173 the receiver during receiver operating hours, while the power block efficiency for simplicity is assumed constant. Thermal
 174 losses and power block efficiency values are retrieved from previous publications (Binotti et al., 2017; Manzolini et al.,
 175 2019; Polimeni et al., 2018). The generated electricity is finally multiplied by the electricity price P_{el} to evaluate the total
 176 plant revenues. Costs related to the operation of the plant and routine maintenance $C_{o\&m}$ in the typical economic approach
 177 (NREL, 2014) are expressed in terms of \$/MWh; therefore, they can directly be subtracted from the electricity price for
 178 an accurate assessment of the actual revenues. The cleaning costs (C_{cl}) are considered separately and expressed more in
 179 detail: they comprise the purchase/rent of the cleaning truck(s) and the hiring of the specialized operators that perform
 180 the cleaning activities. The yearly total profit (TP) is eventually calculated as:

$$TP = \sum_{i=1}^{365} \sum_{j=1}^{N_s} \eta_{opt, clean_{day,ji}}^{day} \cdot f_{soil_{ji}}^{day} \cdot A_j \cdot DNI_{day,i} \cdot \eta_{th,i} \cdot \eta_{pb} \cdot (P_{el} - C_{o\&m}) - C_{cl} \quad (9)$$

181 Where the index i denotes the current day of the year and the index j denotes the sectors of the solar field. Thus,
 182 $\eta_{opt, clean_{day,ji}}$ indicates the average daily optical efficiency of the j -th sector on the i -th day for a perfectly clean solar
 183 field, and $f_{soil_{day,ji}}$ is the correspondent daily soiling factor (that depends on the cleaning schedule).

184 Two scenarios are then considered with regards to the cost of cleaning operations:

- 185 - “owned trucks”, which considers the trucks to be purchased by the plant operator and the truck operators to be
 186 hired for the whole year;
- 187 - “on-call”, which considers the trucks to be rented by the plant operator every time a cleaning is needed, together
 188 with the service of the required truck operators.

189 In the “owned trucks” scenario, the yearly cleaning costs are expressed as:

$$C_{cl} = C_{cl,var} \cdot n_{cl} + C_{cl,fix} \cdot n_{tr} \quad (10)$$

190 where $C_{cl,var}$ represents the variable cleaning costs, n_{cl} the number of cleanings per year, $C_{cl,fix}$ the fixed cleaning costs,
 191 and n_{tr} the number of purchased trucks. The variable cleaning costs account for the water and fuel usage, while the fixed
 192 cleaning costs account for the trucks purchase and maintenance and the salary of the truck operators.

193 In the “on-call” scenario, the yearly cleaning costs are expressed as

$$C_{cl} = C_{cl,rent} \cdot n_{cl} + C_{call} \cdot n_{call} \quad (11)$$

194 where $C_{cl,rent}$ represents the rent cleaning costs, n_{cl} the number of cleanings per year, C_{call} the cost of each cleaning
 195 truck call, and n_{call} the number of truck calls. The rent cleaning costs account for the rental of the trucks, and the payment
 196 of the cleaning shifts performed by the truck operators, while the “call” cost sets a fee that has to be paid every time a
 197 cleaning truck is rented.

198 Since cleaning costs represent only a limited fraction of total operating costs, the adoption of the overall yearly revenues
 199 as described in Eq. (9) as the problem objective function complicates the convergence to the optimal cleaning schedule
 200 since the sensitivity of the objective function with respect to the optimization variables is limited. It is therefore useful to
 201 define an auxiliary objective function that is more representative of the trade-off between cleaning costs and improved
 202 thermodynamic performance, while still accounting for the effect on yearly power plant revenues. This alternative figure

203 of merit is the *total cleaning cost* (TCC), defined as the sum of the actual operating cleaning cost C_{cl} described above in
 204 details and the so-called degradation cost C_{deg} , which accounts for the electricity generation losses due to soiling and is
 205 computed as:

$$C_{deg} = \sum_{i=1}^{365} \sum_{j=1}^{N_s} \eta_{opt, clean, ji}^{day} \cdot (1 - f_{soil, ji}^{day}) \cdot A_j \cdot DNI_{day, i} \cdot \eta_{th, i} \cdot \eta_{pb} \cdot (P_{el} - C_{o\&m}) \quad (12)$$

206 Consequently, the total cleaning cost, which serves as the optimization objective function, is computed as:

$$TCC = C_{cl} + C_{deg} \quad (13)$$

207 Examining Eqs. (9), (12), and (13) it is easy to see that the minimum of TCC corresponds to the maximum of TP.

208

209 **3.1 Heuristic approach**

210 The heuristic approach to cleaning scheduling does not rely on the formal mathematical optimization of the described
 211 problem, but consists in the definition of a rule-based strategy which is then tuned by acting on its characteristic operating
 212 parameters: number of cleaning trucks n_{tr} involved in cleaning operations, and sectorial cleaning interval d^{cl} ,
 213 representing the number of days after which a solar field sector is cleaned again. Every d^{cl} days, all n_{tr} cleaning trucks
 214 are deployed, cleaning the maximum number of sectors every day in a pre-defined order until all solar field sectors have
 215 been cleaned.

216 For a given number of trucks n_{tr} , there will be a minimum cleaning interval d_{min}^{cl} which corresponds to continuously
 217 performing cleaning operations at the maximum rate allowed by the number of deployed trucks. However, cleaning
 218 intervals longer than d_{min}^{cl} might be preferable, since the increase in plant production comes at the expense of the direct
 219 costs associated with the cleaning operations. The heuristic algorithm parameters d^{cl} and n_{tr} are therefore tuned in each
 220 case study by means of a parametric performance assessment: for every admissible combination of n_{tr} and $d^{cl} \in$
 221 $[d_{min}^{cl}, 365]$, the yearly plant performance is evaluated. The optimal combination of cleaning trucks n_{tr} (to be purchased
 222 or rented according to the operating scenario) and sectorial cleaning interval d^{cl} is then simply the combination that
 223 achieves the lowest total cleaning cost. Figure 1a shows the results of the parametric analysis: for each considered number
 224 of trucks n_{tr} the TCC described in Eq. (13) is computed and reported as a function of the annual number of cleanings,
 225 which depends on the cleaning interval d_{cl} . The optimal number of cleanings for a given number of trucks is labelled
 226 with a blue asterisk while the best combination of cleaning interval and number of trucks is labelled with a red bigger
 227 asterisk. The maximum allowable number of trucks and cleanings per year is limited to 8 and 60, respectively, for the
 228 sake of better comprehensibility of the picture. In Figure 1b the TP described in Eq. (9) is displayed as a function of the
 229 annual number of cleanings, which depends on the cleaning interval d_{cl} . The blue and large red asterisks denote,
 230 respectively, the best number of cleanings for each given number of trucks and the overall optimal. The comparison
 231 between Figure 1a and Figure 1b indicates that the same optimal combination of cleaning interval and number of trucks
 232 corresponds to both the maximum total profit (TP) and the minimum total cleaning cost (TCC), as expected.

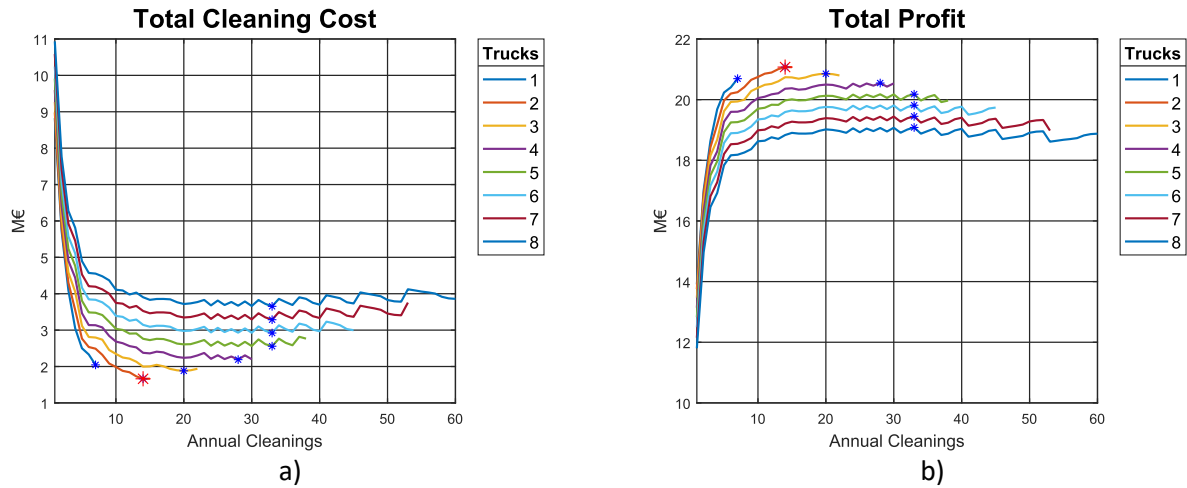


Figure 1. Parametric heuristic algorithm

233

234 The performance of the tuned heuristic approach serves as the benchmark to quantify the advantages deriving from the
 235 proposed advanced approach to cleaning scheduling optimization, via the Mixed Integer Linear Programming (MILP)
 236 model presented in the next section.

237

238 3.2 MILP model

239 Mixed Integer Linear Programming (MILP) denotes a class of optimization problems featuring both integer and
 240 continuous variables and characterized by a linear objective function and linear problem constraints. Many scheduling
 241 optimization problems arising in production planning and logistics are formulated as MILPs because of the following two
 242 substantial advantages:

- 243 - Very efficient solvers are available commercially and they are able to tackle large scale real-world problems;
- 244 - The convexity of the relaxed problem (a linear program where the integrality condition is relaxed) allows
 245 identifying a rigorous assessment of the global optimality of a solution (optimality gap).

246 A MILP formulation of the optimal cleaning scheduling problem was therefore developed, to formally identify the global
 247 optimal scheduling solution that minimize the total cleaning cost (Eq. (13)). It is important to note that the optimization
 248 accounts for the trade-off between increasing cleaning costs due to a higher cleaning frequency and increased plant
 249 productivity. Thus, the global optimum identified by the MILP approach might be associated to higher direct cleaning
 250 costs with respect to the heuristic approach, while obtaining higher yearly revenues by virtue of the enhanced plant
 251 productivity. The independent decision variables of the optimization problem are:

- 252 - the cleaning schedule for each solar field sector, indicating the days of the year in which each sector is to be
 253 cleaned;
- 254 - the number of trucks involved in the cleaning activities (to be purchased/rented).

255 The constraints defining the mathematical formulation of the cleaning scheduling optimization problem are presented
 256 hereafter.

257 Let $\mathcal{S} = \{1, 2, \dots, N_s\}$ be the set of sectors of the solar field and $\mathcal{T} = \{1, 2, \dots, 365\}$ be the set of days in the year. For each
 258 sector $s \in \mathcal{S}$, the binary cleaning scheduling variable $z_{s,\ell,t}$ is equal to 1 if, in day $t \in \mathcal{T}$, mirrors were last cleaned in day
 259 $\ell \in \mathcal{T}$. Variable $z_{s,\ell,t}$ is cyclic in time with respect to temporal index t , representing a periodic cleaning schedule across
 260 consecutive years (i.e., the heliostats' soiling status on the 31st of December represents the day-ahead condition for the 1st

261 of January). The diagonal elements of each bidimensional matrix $z_{s,\ell,t}$ with respect to temporal indexes t and ℓ
 262 (henceforth referred to as $Z^s \subseteq \mathbb{R}^{365 \times 365}$), or equivalently all variables $z_{s,\ell,t}$ with $t = \ell$, assume the value 1 if the sector
 263 was last cleaned that same day. They therefore represent the cleaning schedule of sector s . In each day $t \in \mathcal{T}$ and for each
 264 sector $s \in \mathcal{S}$, it is possible to univocally identify a single day in which the sector was last cleaned as:

$$\sum_{\ell \in \mathcal{T}} z_{s,\ell,t} = 1 \quad \forall s \in \mathcal{S}, t \in \mathcal{T} \quad (14)$$

265 On the other hand, if the mirrors were not cleaned on a given day $\hat{\ell} \in \mathcal{T}$ (i.e. $z_{s,\hat{\ell},\hat{\ell}} = 0$), all variables $z_{s,\ell,t}$ must be equal
 266 to zero since sector s was never cleaned during day $\hat{\ell}$:

$$z_{s,\ell,\hat{\ell}} \cdot 365 \geq \sum_{t \in \mathcal{T}} z_{s,\ell,t} \quad \forall s \in \mathcal{S}, \ell \in \mathcal{T} \quad (15)$$

267 With each cleaning scheduling variable $z_{s,\ell,t}$ is associated the parameter $\tilde{f}_{s,\ell,t}$, which indicates the soiling factor for the
 268 mirrors of sector s in day t , in case they were last cleaned in day ℓ . All potential soiling factors $\tilde{f}_{s,\ell,t}$ are computed
 269 according to the soiling model described in (Picotti et al., 2018). The actual sector soiling factor $f_{soil_{ji}}^{day}$ associated to the
 270 scheduling plan $z_{s,\ell,t}$ can be therefore calculated, in each day $t \in \mathcal{T}$, as:

$$f_{soil_{ji}}^{day} = \sum_{\ell \in \mathcal{T}} z_{s,\ell,t} \tilde{f}_{s,\ell,t} \quad \forall s \in \mathcal{S}, t \in \mathcal{T} \quad (16)$$

271 Constraint (14) already implies that one and only one of all potential soiling factor values $\tilde{f}_{s,\ell,t}$ must be considered in each
 272 day t , or in other words that for each column t only one of the rows ℓ can have a non-zero value of $z_{s,\ell,t}$. Optimality of
 273 the solution will imply that, within the pool of “active” rows (non-zero diagonal variable $z_{s,\ell,\ell}$, constraint (15)) will be
 274 selected the one associated to the lowest soiling factor $\tilde{f}_{s,\ell,t}$. If the optimal solution features a cleaning operation of the
 275 sector on day ℓ , the active variable will be the diagonal variable $z_{s,\ell,\ell}$, otherwise it will be the variable $z_{s,\ell,t}$ with the
 276 lowest non-negative difference $\ell - t$ (accounting for the cyclicity of temporal indexes). To speed up convergence (by
 277 tightening the problem formulation) it is useful to introduce an additional constraint which tends to “group” the non-zero
 278 entries in the matrix Z^s , and guide the solution algorithm towards the optimal variables configuration:

$$z_{s,\ell,t} \leq z_{s,\ell,t-1} \quad \forall s \in \mathcal{S}, t, \ell \in \mathcal{T}, t \neq \ell \quad (17)$$

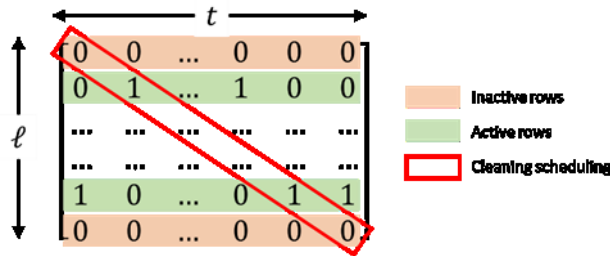


Figure 2. Cleaning scheduling matrix Z^s for sector $s \in \mathcal{S}$

281 A visual interpretation of matrix Z^s is provided in Figure 2: for a given sector, each column t of Z^s is associated to a day
 282 of the year, while each row ℓ represents the last day of the year, from the temporal perspective of t , in which s was
 283 cleaned. The diagonal of Z^s is the cleaning schedule of sector s , and each of its elements $z_{s,\ell,\ell}$ activates the corresponding
 284 binary variables on the ℓ^{th} row.

285 The sum of diagonal elements of all matrixes Z^s yields a vector whose elements indicate the number of cleaning
 286 operations taking place in a given day, which correspond to the number of trucks (according to the assumption that the
 287 sectors are sized such that one crew operating one truck cleans one sector per day). In the “owned trucks” scenario, the
 288 maximum number of simultaneous cleaning operations determines the requirement in terms of purchased cleaning trucks:

$$\sum_{s \in \mathcal{S}} z_{s,t,t} \leq n_{tr} \quad \forall t \in \mathcal{T} \quad (18)$$

289 As for the “on call” scenario, a fixed cost must be paid each time new trucks are called to take part in the cleaning
 290 operations (Eq. (11)). To account for the fixed call cost in the MILP formulation objective function, it is necessary to
 291 introduce the non-negative integer variable c_t , equal to the number of new trucks which were not present the day before
 292 that are performing cleaning duties during day $t \in \mathcal{T}$:

$$c_t \geq \sum_{s \in \mathcal{S}} z_{s,t,t} - \sum_{s \in \mathcal{S}} z_{s,t-1,t-1} \quad \forall t \in \mathcal{T} \quad (19)$$

293 The number of yearly truck calls is thus equal to the summation of c_t :

$$n_{call} = \sum_{t \in \mathcal{T}} c_t \quad (20)$$

294 The optimization problem is formulated in MATLAB, using the extension YALMIP (Lofberg, 2004), and it is solved
 295 using the commercially available solver GUROBI (Guorobi Optimization, 2018).

296

297 **4 Case studies**

298

299 The heuristic and deterministic optimization methodologies were applied to two ST plants located in Woomera in South
 300 Australia (31°12'S 136°48'E) and in Abu Dhabi in the United Arab Emirates (24°24'N 54°42'E). The two areas were
 301 selected as they have different characteristics in terms of latitude, climate, and airborne dust concentration.

302 Two different solar fields were generated using SolarPilot (NREL, 2017) assuming 700 MW as target power on the
 303 receiver on the summer solstice. Receiver geometry, tower height and heliostats size were set according to literature data
 304 for the Crescent Dunes plant (Mehos et al., 2017; SolarReserve), while heliostat total reflected image error was assumed
 305 equal to the SolarPilot default value of 3.07 mrad. The two simulated solar fields, the related sectors, and the representative
 306 heliostat for each sector (red dots) are represented in Figure 3. The characteristics of the two heliostats fields are reported
 307 in Table 1, together with their performance on the summer solstice.

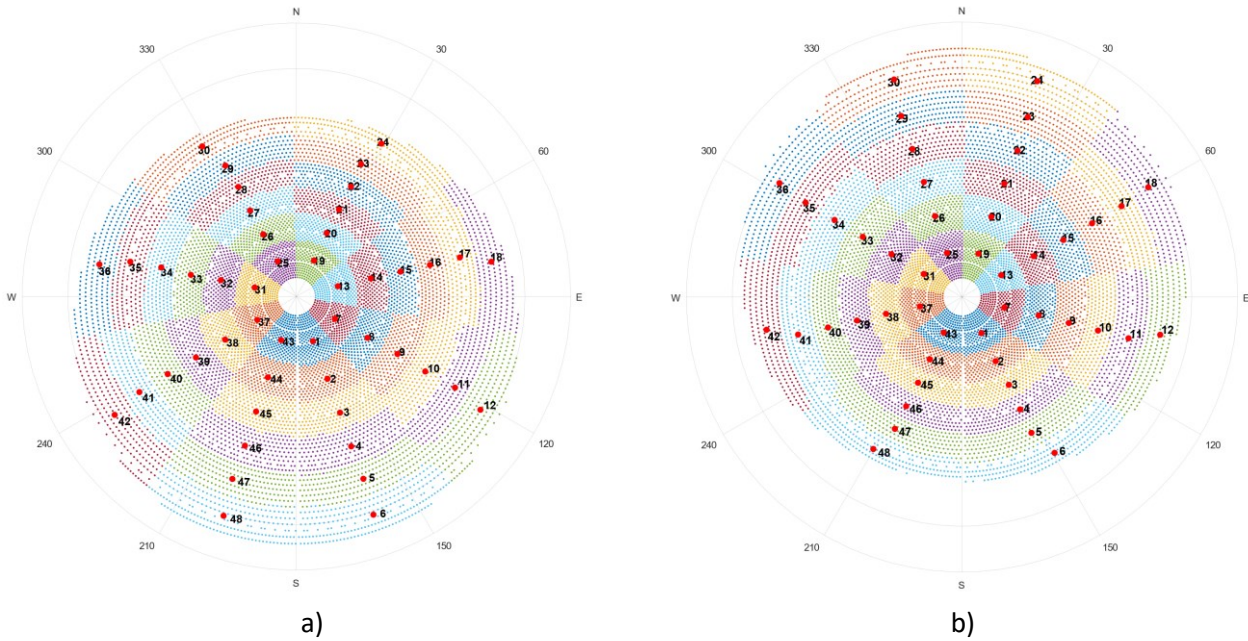


Figure 3. Solar field a) Woomera ; b) Abu Dhabi

Table 1 – Solar field design assumptions and performances

Design Assumptions		
Direct Normal Irradiation [W/m ²]	900	
Location	Abu Dhabi	Woomera
Geographical Coordinates	24°24'N 54°42'E	31°12'S 136°48'E
HTF type	Solar Salts	Solar Salts
Receiver size		
Height [m]	30.5	30.5
Diameter [m]	15.8	15.8
Tower height [m]	195	195
Field type	Surrounded	Surrounded
Minimum radius of the field [m]	126.7	126.7
Maximum radius of the field [m]	1626	1626
Number of heliostats	10328	10336
Heliostat size [m ²]	11.3 x 10.4	11.3 x 10.4
Heliostat reflectivity	0.95	0.95
Heliostat total reflected image error [mrad]	3.07	3.07
Performance		
Sun Position		
Zenith	0.95	7.75
Azimuth	180	0
Optical efficiency	0.652	0.651
Power on the receiver [MW]	701.6	701.2
Receiver thermal losses [MW]	105	105
Power block efficiency	0.35	0.35

308

309

310

311 The number of sectors considered for the two case studies is 48, with 6 radial and 8 angular partitions in order to have
 312 similar values of optical efficiency within the sectors. This provided sectors made of the same number of heliostats (± 1)
 313 such that each could be cleaned in one day (12 working hours) using one truck. The average cleaning speed of 2000 m²/h
 314 has been assumed as a reasonable value within the cleaning speed range reported in Pfahl et al. (2017). Moreover, it is a
 315 good compromise between computational efforts and accuracy of the model. A higher number of sectors would greatly
 316 increase the computational time of the optimization, while a smaller number of them would hinder the effectiveness of
 317 the optimization as the sectors would include heliostats whose soiling factor and optical efficiency could differ

318 significantly. A parametric analysis on the influence that different cleaning speeds and sectorizations of the solar field
 319 have on the outcomes of the optimization is discussed in Section 5.1.2.

320 For each sector, the nominal optical efficiency $\eta_{opt, clean}$ assigned to the sector representative heliostat located in its
 321 geometrical barycentre is computed as the average “as-clean” optical efficiency of all the heliostats composing it.

322 The cleaning strategy optimizations were performed for the two selected sites on hourly time step to calculate the optical
 323 efficiency and actual thermal energy on the receiver. The time step coincides with the availability of the environmental
 324 conditions measured by the local weather stations. The one located in Woomera provides data regarding DNI, wind speed,
 325 and air temperature. Since data about dust concentration are not locally available for the Australian site, PM10 (particulate
 326 matter whose aerodynamic diameter is smaller than $10\mu\text{m}$) measurements are obtained from the location of Moolawatana,
 327 in SA, as the climate and the environmental characteristics are similar to Woomera. The PM10 data are adapted to fit in
 328 the assumed dust size distribution, chosen as ‘rural’ from Seinfeld and Pandis (1998), to be as close as possible to the
 329 simulated environment. Weather data for Abu Dhabi are obtained from the SolarPILOT database while the average
 330 monthly dust concentration measured in Mushrif Park (UAE) is used to scale the hourly dust concentration measured in
 331 Moolawatana.

332 The main economic parameters are reported in Table 2 for both “owned trucks” and “on call” cost structures. Finally,
 333 given the size of the heliostats, the number of heliostats per sector, and the cleaning speed, it is assumed that a cleaning
 334 operation requires two six-hours-shifts of a team made by two operators who operate a truck. Each cleaning crew
 335 composed by 4 operators and a truck is then able to clean one sector per day.

336 *Table 2. Economic assumptions*

	“owned trucks”	“on call”
Truck operator salary [\$/yr]	80000	-
Truck operator hiring [\$/day]	-	250
Truck rent cost [\$/day]	-	250
Truck purchase cost [\$]	150000	-
Truck maintenance cost [\$/yr]	15000	-
Water and fuel cost [\$/m ²]	0.01	-
Call cost [\$/call]	-	1000
Depreciation time [yr]	4	-
Electricity price [\$/MWh]	50	50

337
 338 To further demonstrate the capabilities of the model and assess the scheduling impact of different locations, different
 339 values of airborne dust concentration were used, as well as different economic assumptions regarding the selling price of
 340 electricity: the measured PM10 values have been halved, increased five and ten times, while the electricity price has been
 341 increased and decreased by 50%. The whole set of performed scenarios (including the two base cases) is summarized in
 342 Table 3.

343 *Table 3. Cleaning optimization scenarios*

Location	Electricity Price [\$/MWh]	Average PM10 [$\mu\text{g}/\text{m}^3$]
Woomera	50	4.441
Abu Dhabi	50	126.315
Woomera x 0.5	50	2.220
Woomera x 5	50	22.203
Woomera x 10	50	44.406

Woomera LP	25	4.441
Woomera HP	75	4.441

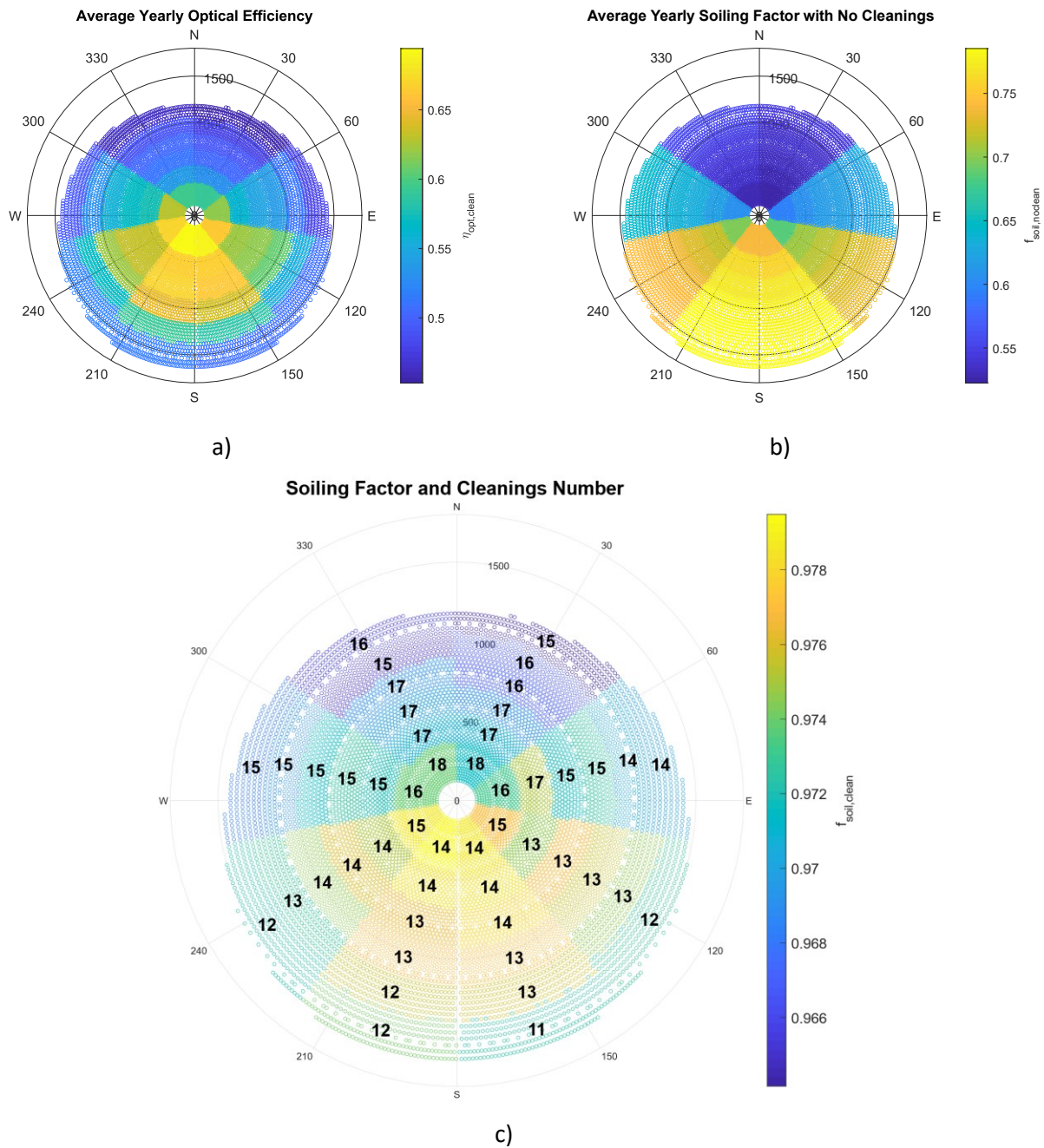
344

345 **5 Results**

346

347 For the base case of Woomera, the reduction of Total Cleaning Cost (TCC) for the MILP compared to the heuristic
348 approach is 3.75% (62.4k\$) for the “owned trucks” scenario and 15.39% (245.1 k\$) for the “on call” scenario. Figure 4
349 illustrates the outcomes of the MILP cleaning optimization for the “owned trucks” case for Woomera. Figure 4a shows
350 the average yearly optical efficiency ($\eta_{opt, clean}$) of each sector of the field, computed as the average “as-clean” optical
351 efficiency of all the heliostats composing each sector, while Figure 4b represents the corresponding average yearly soiling
352 factor without cleanings ($f_{soil, noclean}$), computed for each sector-representative heliostat and then applied to all the
353 heliostats belonging to the same sector. Figure 4c finally depicts the results of the MILP optimization. The number of
354 annual cleanings for each sector is displayed in the sector’s geometrical barycentre. The resulting average yearly soiling
355 factor ($f_{soil, clean}$) is also illustrated through the colour map.

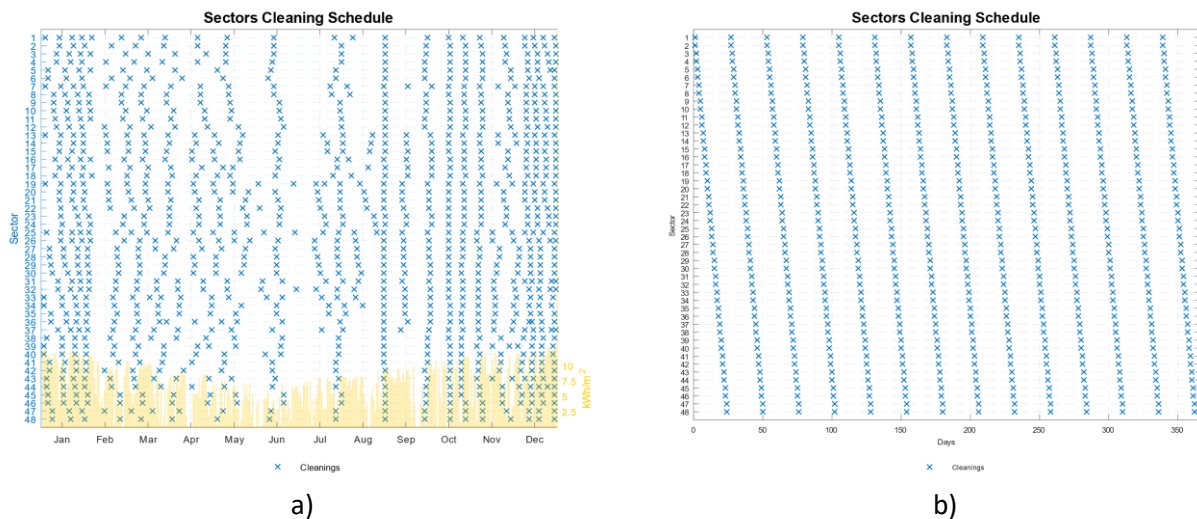
356



357 Figure 4. Cleaning summary and impact - Woomera - "owned trucks"; a) Average yearly optical efficiency ; b) Average yearly soiling
 358 factor without cleanings ; c) Optimization outcomes

359 It is worth noting that the sectors that are cleaned more frequently have either high yearly average optical efficiency
 360 (especially those sectors that are close to the tower) or low average yearly soiling factors without cleanings $f_{soil, noclean}$
 361 (i.e. they are subjected to more soiling). The resulting lower yearly average soiling factor ($f_{soil, clean}$ in Figure 4c) occurs
 362 in the sectors with the lower yearly average optical "as-clean" efficiency, despite the high cleaning frequency, as it may
 363 be noticed looking at the darker tonalities in the upper part of the graph in Figure 4c. This is in agreement with their
 364 smaller contribution in terms of thermal power reflected onto the receiver. It is also possible to recognize that the sectors
 365 with the lower $f_{soil, noclean}$ are the ones located further in the northern part of the solar field (in a ST plant located in the
 366 Southern Hemisphere). This can be explained by the lower average tilt angles of these heliostats, leading to higher soiling
 367 rates, in accordance to the model developed in Picotti et al (2018). Besides the annual number of cleanings and trucks
 368 required, the precise cleaning scheduling and timing is the most peculiar aspect of the MILP optimization: Figure 5a

369 shows the cleaning events for each sector along the whole year (sector numbers refer to Figure 3). It can be seen the
 370 higher cleaning frequency of either the sectors closer to the tower or the northerner sectors is in accordance to Figure 4c.
 371 It is also interesting to note that the cleaning frequency is higher during summer (December to February in Australia),
 372 when the available DNI, the overall “as-clean” optical efficiency, and the receiver thermal efficiency are higher, and
 373 lower during winter (June to August in Australia), when the available DNI, the overall “as-clean” optical efficiency, and
 374 the receiver thermal efficiency are lower.
 375



376 *Figure 5. Cleaning schedule – Woomera – “owned trucks”: a) MILP ; b) Heuristic*

377 The corresponding cleaning schedule for the heuristic approach is displayed in Figure 5b. It is clearly observable the
 378 cleaning pattern is much more regular, which regardless of the different soiling factor and optical efficiency of the various
 379 sectors suggests cleaning each sector 14 times per year. Although both approaches assess that the optimal number of
 380 cleaning trucks is two, the number of annual cleanings is higher for the MILP optimization (699 vs 672). This results in
 381 higher direct cleaning costs, but the enhanced optical efficiency leads to a higher power generation, lower TCC, and
 382 higher profit. The superiority of the MILP approach resides in the smarter allocation of the cleanings, increasing their
 383 frequency during high-productivity periods for those sectors that are more soiled or with higher “as-clean” optical
 384 efficiency and decreasing their frequency when they are less needed. Overall, for the analysed case, the MILP approach
 385 reduces the TCC by 3.75%.

386 When considering the “on call” policy for the same case, the economic advantage of the MILP solution over the heuristic
 387 increases, owing to the higher degrees of freedom of this policy. Although the number of calls is increased from 42 to 58,
 388 the number of cleanings is reduced from 672 to 526, and savings on both the degradation cost and the direct cleaning
 389 operations is obtained by allocating the cleanings in the most suitable times. Figure 6a and Figure 6b allow a visual
 390 comparison between the MILP and heuristic optimal cleaning schedules, outlining the more scattered optimal strategy of
 391 the MILP approach which yields a significant 15.39% decrease of the TCC.

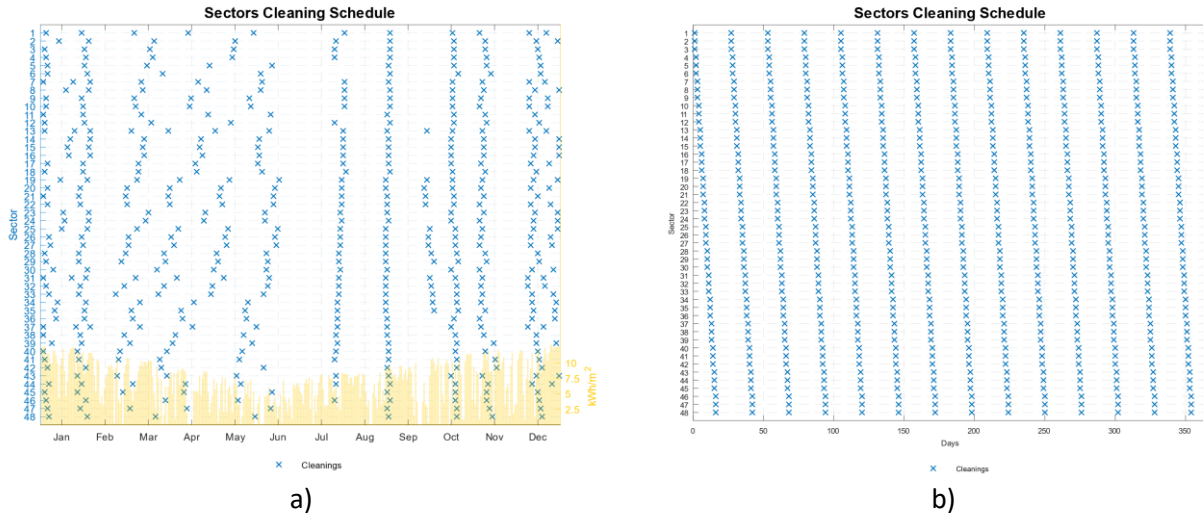
392 Table 4 reports the monthly values of DNI and average airborne dust concentration, together with the related number of
 393 cleanings, to highlight their efficient scheduling obtained with the MILP optimization for both the “owned trucks” and
 394 “on call” scenarios. As the latter has a higher flexibility regarding the deployment of cleaning trucks, the difference
 395 between winter and summer months is much higher.

396 A summary of the comparison between the MILP and the heuristic cleaning optimization for the two scenarios is reported
 397 in Table 5.

398 Table 4. Monthly cleanings summary – Woomera

	Jan	Feb	Mar	Apr	May	Jun	Jul	Aug	Sep	Oct	Nov	Dec
“owned trucks”	60	56	62	60	55	51	49	62	60	62	60	62
“on call”	79	28	49	31	31	30	30	23	43	56	48	78
DNI [kWh/m ²]	328	211	220	171	143	107	166	189	191	240	235	304
Dust Concentration [μg/m ³]	4.0	2.4	3.0	4.7	3.4	1.8	4.2	5.5	2.8	5.4	3.7	11.8

399



400

Figure 6. Cleaning schedule – Woomera – “on call”: a) MILP ; b) Heuristic

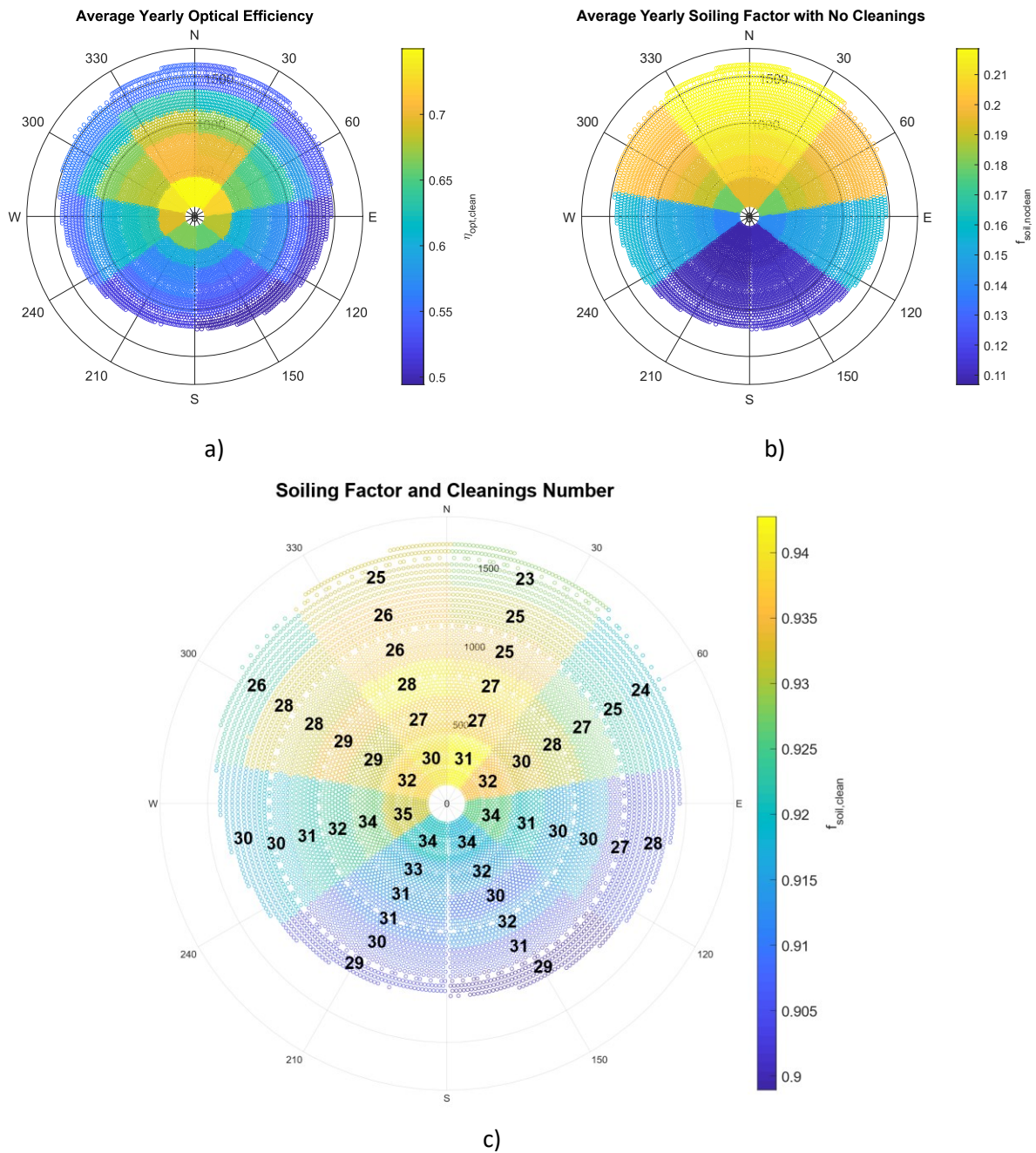
401 Table 5. MILP vs Heuristic comparison summary – Woomera

	“owned trucks”		“on call”	
	MILP	Heuristic	MILP	Heuristic
Trucks/Calls	2	2	58	42
Cleanings	699	672	526	672
C _{cl} [k\$/yr]	919.2	912.5	715.1	881.5
C _{deg} [k\$/yr]	680.9	750.1	633.0	711.7
TCC [M\$/yr]	1.60	1.66	1.35	1.59
TP [M\$/yr]	21.14	21.07	21.39	21.14

402

403 The cleaning optimization was also applied to the case study of Abu Dhabi. The TCC improvement (reduction) of the
 404 MILP versus the heuristic approach for the “owned trucks” and “on call” policies is 0.68% (26.3 k\$) and 12.15% (477.5
 405 k\$), respectively. Figure 7 illustrates the outcomes of the MILP cleaning optimization for the “on call” case. Similar to
 406 the Woomera case, the most frequently cleaned sectors are those whose yearly average optical efficiency is higher (Figure
 407 7a) or whose soiling factor with no cleanings ($f_{soil, noclean}$) is lower (Figure 7b). However, since Abu Dhabi is in the
 408 Northern Hemisphere, the location of the heliostats with lower average tilt angles (i.e. the most soiled ones) are in the
 409 southern part of the solar field. Due to the much higher average airborne dust concentration in the UAE compared to
 410 South Australia, the number of cleanings per sector is considerably higher (see also the significantly lower average yearly
 411 soiling factor with no cleanings $f_{soil, noclean}$).

412



413 *Figure 7. Cleaning summary and impact – Abu Dhabi – “on call”: a) Average yearly optical efficiency ; b) Average yearly soiling*
 414 *factor without cleanings ; c) Optimization outcomes*

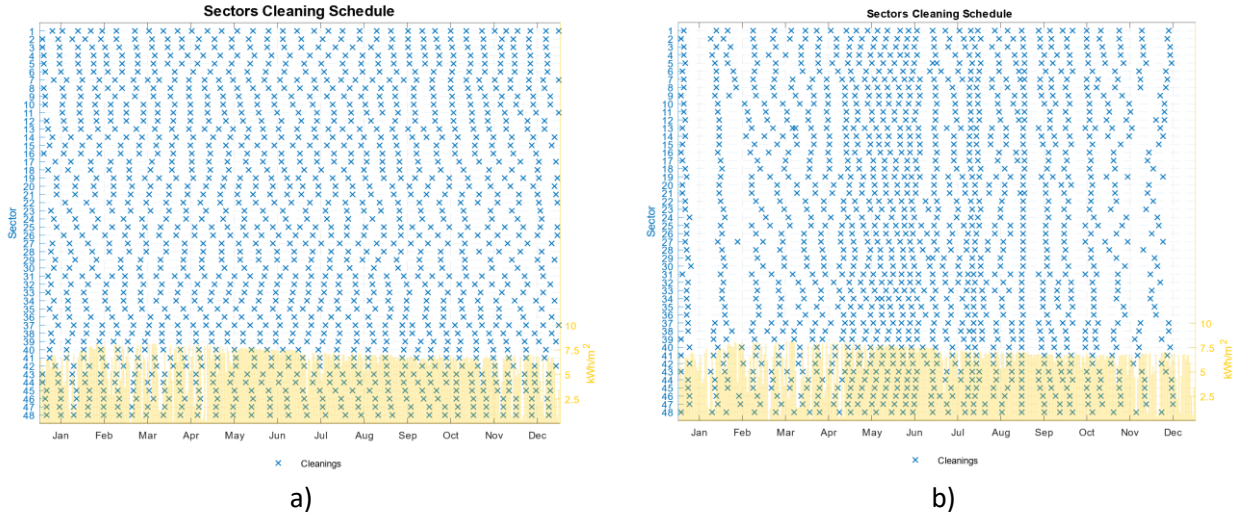
415 As for the optimization performed for the location of Woomera, summer months (June to August in the UAE) experience
 416 the higher cleaning frequency, especially for the “on call” scenario, as reported in Table 6. The increased cleaning
 417 frequency is due to the higher airborne dust concentration measured in Abu Dhabi.

418 The graphical representation of the detailed cleaning schedules depicted in Figure 8 also confirms the described trend,
 419 emphasizing the more frequent cleaning of the southernmost heliostats and during summer (more clearly visible in Figure
 420 8b).

421 Table 6. Monthly cleanings summary – Abu Dhabi

	Jan	Feb	Mar	Apr	May	Jun	Jul	Aug	Sep	Oct	Nov	Dec
“owned trucks”	148	138	155	150	155	150	155	155	150	155	147	118
“on call”	88	75	102	127	186	177	168	129	121	114	78	41
DNI [kWh/m ²]	171	188	160	173	230	225	201	208	206	208	181	162
Dust concentration [μg/m ³]	111	101	103	150	135	145	178	154	140	116	91	90

422



423

Figure 8. Cleaning schedule – Abu Dhabi: a) “owned trucks”; b) “on call”

424 Compared to the heuristic approach, the MILP optimization of the “owned trucks” cleaning strategy improves the TCC
 425 by smartly allocating the significantly increased number of cleanings and decreasing the number of trucks. In the “on
 426 call” case, the MILP optimization both creates better ‘clusters’ of continuous cleanings to diminish the number of truck
 427 calls (n_{call} in Eq. (11)), and also intensify the cleanings when and where they are more needed, thus reducing both the
 428 operational and degradation related cleaning costs, and hence the TCC. Table 7 summarizes the main parameters of the
 429 cleaning optimizations performed for the case of Abu Dhabi.

430 Table 7. MILP vs Heuristic comparison summary – Abu Dhabi

	“owned trucks”		“on call”	
	MILP	Heuristic	MILP	Heuristic
Trucks/Calls	4	5	92	145
Cleanings	1446	1824	1406	1392
C_{cl} [k\$/yr]	1850.0.	2316.7	1848.1	1883.6
C_{deg} [k\$/yr]	1970.7	1530.4	1603.7	2045.7
TCC [M\$/yr]	3.82	3.85	3.45	3.93
TP [M\$/yr]	17.90	17.87	18.27	17.79

431

432 5.1 Sensitivity analysis

433 The optimization scheme for the two scenarios described in the previous section has been applied to the base case of
 434 Woomera for different dust concentrations and electricity prices (see Table 3), and solar field sectorizations (see Table
 435 10). The outcomes of such sensitivity analyses are described and analysed in the following sub-sections.

436 5.1.1 Dust concentration and price variations

437 The airborne dust concentration is a parameter of paramount importance when evaluating the soiling-related optical
 438 efficiency losses of the heliostats since it strongly affects the amount of dust that is deposited on the reflective surfaces.

439 The values measured in Moolawatana and adopted for the base case of Woomera have been halved, increased 5 and 10
 440 times, to properly assess the relevance they have on the outcomes of the optimization.

441 For both “owned trucks” and “on call” scenarios, the share of the TCC on the TP increases as the dust concentration is
 442 increased, as reported in Table 8 and Table 9. This reflects the necessity for more frequent cleanings in dustier
 443 environments. Since the TCC is more relevant for the scenarios that consider higher concentration of dust in air, its
 444 improvement has a more relevant impact on the total profit of the plant: as reported in Table 8, considering the “owned
 445 trucks” scenario, the TCC decrease obtained with the MILP optimization is larger for the lowest-dust case (7.43%) than
 446 for the highest-dust case (4.60%). Nevertheless, the impact on the total profit is 0.43% for the former, and 1.29 % for the
 447 latter, since the impact of the TCC on the TP grows from 5.36% to 26.37%, respectively. The same trend is observed for
 448 the corresponding cases in the “on call” scenario, as summarized in Table 9.

449 As expected, the higher the dust concentration in air, the higher is the number of trucks purchased or called, as well as
 450 the number of cleanings per year. Concerning the “owned trucks” scenario, Table 8 shows that for the four dust
 451 concentrations analysed, the trucks number grows from just 1 to 6, as the annual cleanings rise from 364 to 2054.
 452 Coherently for the “on call” scenario, Table 9 shows that the number of calls grows for 40 to 194, as the annual cleanings
 453 rise from 379 to 1597. Figure 9a and Figure 9b depict the cleaning schedules for the lowest-dust and highest-dust cases
 454 for the “owned trucks” scenario. It is remarkable to observe that once again the cleanings are less frequent during winter
 455 (June to August in South Australia), and the northernmost sectors require an higher number of cleanings.

456 Moving to the sensitivity analysis on the price of electricity, the HP case has a higher number of cleanings and higher
 457 number of trucks purchased/called. This reflects the better convenience of investing more money for cleaning operations
 458 to generate more electricity and more profit. The opposite occurs when the electricity price is lower. Figure 10a and Figure
 459 10b depict the cleaning schedules for the LP and HP cases, clearly showing the higher cleaning frequency in the second
 460 case. A comprehensive summary of the main parameters for all the sensitivity analyses described in this section is reported
 461 in Table 8 and Table 9. The results of these analyses stress the importance of developing optimized cleaning strategies as
 462 they vary from case to case. In addition, the developed optimization algorithm always significantly improves the TCC
 463 and thus the profit of the plant. Finally, Table 8 and Table 9 report the computational time required for each case. The
 464 optimizations were performed on a Windows virtual machine with 16 virtual processors (2.3 GHz of standard frequency)
 465 of an Intel® Xeon® E5-2686 v4 CPU chipset and 122 Gib of RAM.

466 *Table 8. Sensitivity analysis summary - "owned trucks"*

	Owned Trucks					
	Woomera	Woomera x0.5	Woomera x5	Woomera x10	Woomera HP	Woomera LP
Tot Profit [M\$/y]	21.14	21.58	19.31	17.99	32.99	9.41
TCC [M\$/y]	1.60	1.16	3.43	4.74	1.97	1.11
C _{cl} [k\$/y]	919.2	463.2	1840.1	2746.8	923.7	463.2
C _{deg} [k\$/y]	680.9	694.2	1590.4	1997.2	1040.9	641.9
Electricity [GWh/y]	474.3	474.0	454.7	446.0	474.4	459.1
N TRUCKS	2	1	4	6	2	1
N CLEANS	699	364	1405	2054	717	364
TP INCREASE	0.30%	0.43%	0.88%	1.29%	0.30%	0.92%
TCC DECREASE	3.75%	7.43%	4.69%	4.60%	4.82%	7.18%
TCC share on TP	7.57%	5.36%	17.77%	26.37%	5.95%	11.75%

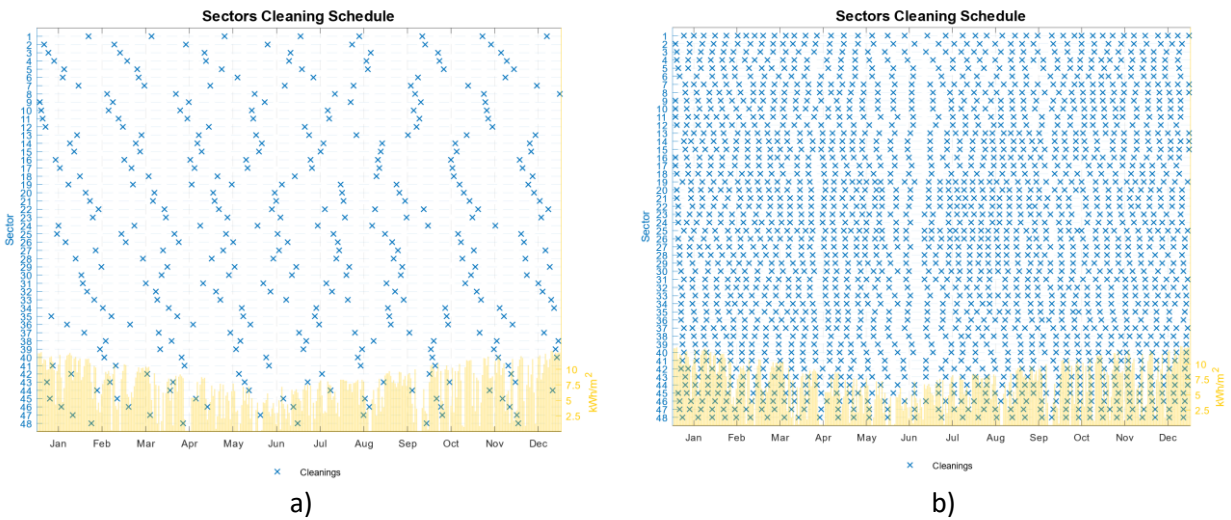
Computational time [s]	793056	3061385	18184	26322	293784	4525604
------------------------	--------	---------	-------	-------	--------	---------

467

468 Table 9. Sensitivity analysis summary - "on call"

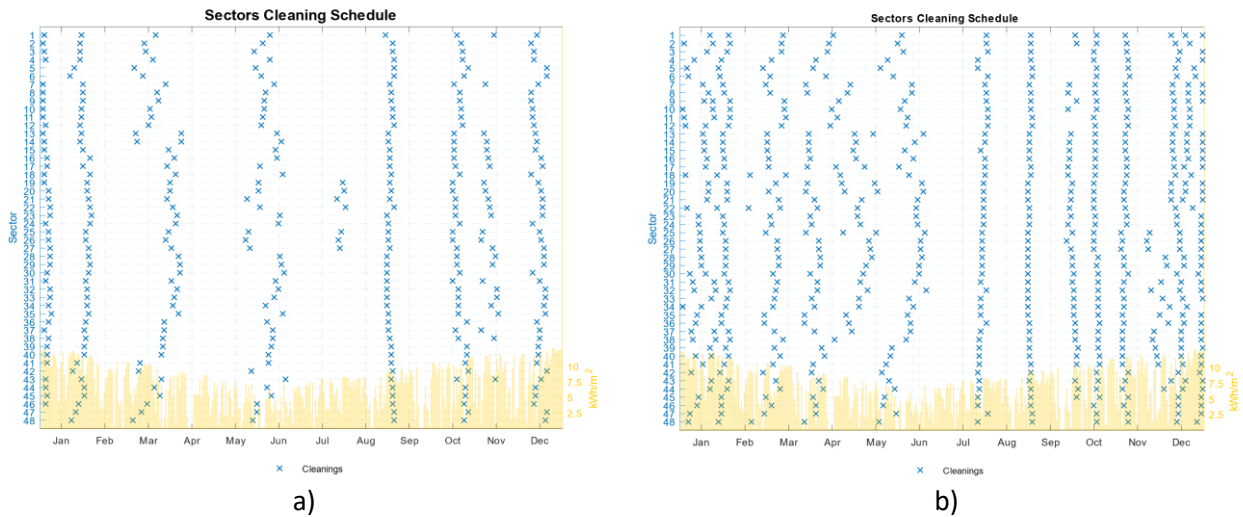
	On Call					
	Woomera	Woomera x0.5	Woomera x5	Woomera x10	Woomera HP	Woomera LP
Tot Profit [M\$/y]	21.39	21.77	19.83	18.72	33.31	9.59
TCC [M\$/y]	1.35	0.96	2.90	4.01	1.65	0.93
C _{cl} [k\$/y]	715.1	513.4	1567.1	2188.9	882.5	492.0
C _{deg} [k\$/y]	633.0	448.7	1334.1	1822.1	770.9	435.4
Electricity [GWh/y]	475.3	479.3	460.2	449.8	478.2	468.7
N CALLS	58	40	153	194	83	36
N CLEANS	526	379	1132	1597	640	365
TP INCREASE	1.16%	0.94%	3.69%	5.50%	0.98%	1.91%
TCC DECREASE	15.39%	17.37%	19.55%	19.59%	16.32%	16.20%
TCC share on TP	6.30%	4.42%	14.63%	21.42%	4.96%	9.67%
Computational time [s]	425087	619714	44906	8092	130930	383971

469



470 Figure 9. Cleaning schedule – Woomera - "owned trucks": a) lowest dust concentration (x 0.5) ; b) highest dust concentration (x10)

471

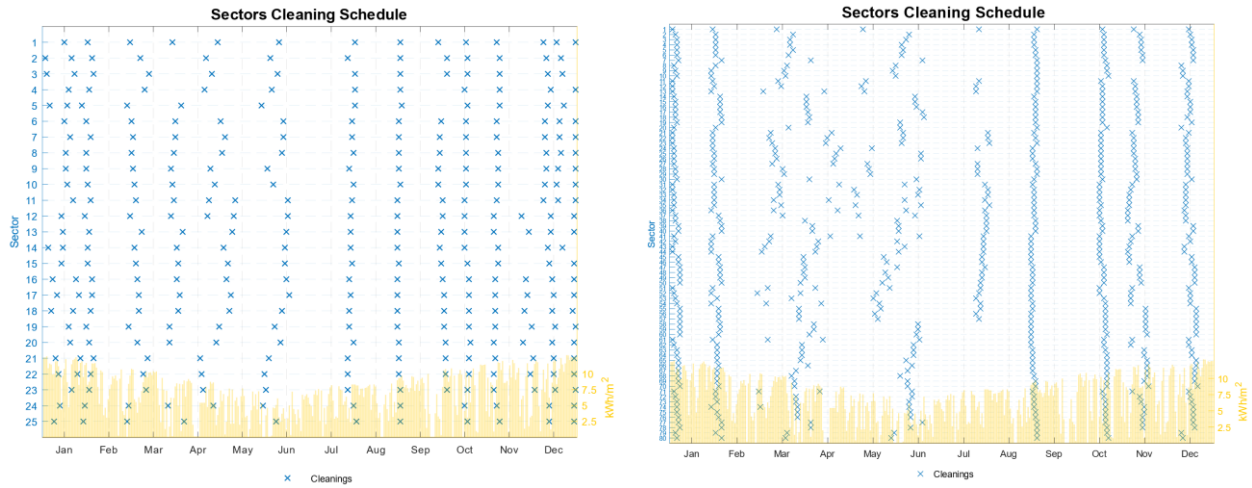


472 Figure 10. Cleaning schedule – Woomera - "on call": a) low electricity price (- 50%) ; b) high electricity price (+ 50%)

473 **5.1.2 Solar field sectorizations**

474 The size and the number of the sectors through which the solar field has been divided to perform the optimization of the
 475 cleaning schedule have been chosen according to the reasons explained in Section 4. However, for the sake of
 476 completeness, it is worth considering that technological and design constraints or the exploitation of different cleaning
 477 technologies could lead to higher or lower cleaning speeds, as well as cleaning patterns that would impose a different
 478 configuration of the sectors. The impact of these aspect on the cleaning optimization is assessed hereafter.

479 To evaluate the effect of the cleaning speed on the optimal cleaning schedule, the extremes of the range proposed by Pfahl
 480 et al. (2017) have been adopted for the “on call” scenario: the maximum value is 3750 m²/h and the minimum value is
 481 1250 m²/h. The corresponding number of sectors whose area equals one truck daily cleaning capability is about 25 (5
 482 radial and 5 angular partitions) and 80 (10 radial and 8 angular partitions), respectively. Although it is expected that higher
 483 cleaning speeds would incur higher costs per square meter (or lower cleaning effectiveness), the same economic
 484 assumption reported in Table 2 are applied since a detailed modelling of the relationship between cost/cleaning speed and
 485 cleaning effectiveness is outside the scope of this study. As reported in Table 10, the higher cleaning speed results in a
 486 lower TTC since the heliostats can be cleaned more often with low extra cost while a lower cleaning speed sensibly
 487 increases the TTC since an higher number of cleaning shifts is required to maintain the optimal soiling factor. The optimal
 488 cleaning schedule for each of the two considered cleaning speeds is depicted in Figure 11.



a)

b)

489

Figure 11. Cleaning schedule – Woomera - "on call": a) high cleaning speed ; b) low cleaning speed

490

Finally, two additional sectorial configurations are considered, changing the number of radial and angular partitions of the solar field while keeping the same number of heliostats per sector (and hence total number of sectors). The analysis is performed only on the “on call” case for the location of Woomera. The variation of the total cleaning cost obtained through the MILP model for these two configurations with respect to the base case is reported in Table 10. The results are very similar to the base case, however the TCC slightly increases when adopting unbalanced sectorizations (i.e. much higher/lower number of radial vs angular partitions). This is due to the higher error made by assuming the whole sector to behave (in terms of soiling factor and optical efficiency) as its representative heliostat (highlighted by red dots in Figure 12). Finally, the computational time for each case is also reported in Table 10. It can be noted that as the number of sectors increases, so does the time required to run the optimization.

496

499

Table 10. Sectorization analysis outcomes

Sectors (Radial x Angular)	Cleaning Speed [m ² /h]	TCC [k\$]	ΔTCC [k\$]	ΔTCC [%]	Number of Cleanings	Computational time [s]
6 x 8 (base case)	2000	1348.0	-	-	526	425087
10 x 8	1250	1682.5	334.5	24.82%	698	750911
5 x 5	3750	1041.1	-306.9	-22.77%	341	53201
16 x 3	2000	1348.6	0.6	0.04%	519	391880
2 x 24	2000	1349.2	1.2	0.09%	520	537412

500

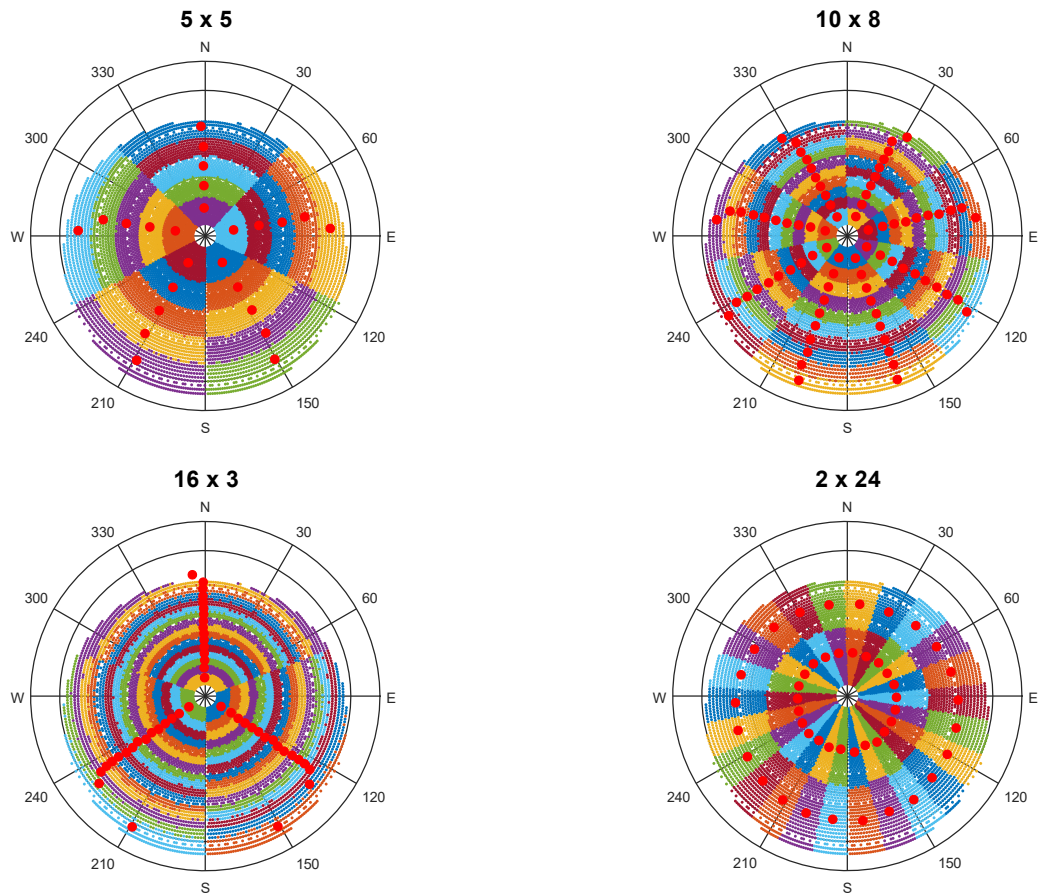


Figure 12. Solar field sectorizations

501

502

503 6 Conclusions

504

505 The most suitable sites for the deployment of ST plants are usually arid and desert areas, where the available DNI is very
 506 high and precipitations are low, while dust or sand events are frequent. These environmental conditions are likely to cause
 507 significant reduction of the optical efficiency of the heliostats composing the solar field, hence reducing the power
 508 generation. The resulting lower profits in turn would hinder the ST plants competitiveness in the energy market. Artificial
 509 cleaning of the solar field is then mandatory to improve the productivity of a ST plant. The optimization of the cleaning
 510 activities is fundamental to achieve better performance and to lower the Levelized Cost of Electricity. This paper
 511 presented the development of an innovative optimization method of heliostat cleaning strategies through a Mixed Integer
 512 Linear Programming (MILP) model. The optimization relies on a validated physical model for solar collectors soiling
 513 which provides the optical efficiency losses in the different sectors of the solar field: the outcomes of the soiling model
 514 depict a very inhomogeneous optical efficiency loss around the solar field, which further states the relevance of a cleaning
 515 scheduling that properly considers the different and time-varying cleaning frequency for each sector of the solar field.
 516 The developed algorithm maximizes the revenues of a ST plant by minimizing the costs related to cleaning activities and
 517 soiling losses. In addition, a simple heuristic optimization is proposed and compared to the results achieved with the MILP
 518 model.

519 For the base case of Woomera analysed in this study, the results of the optimization show a significant potential for
 520 reduction of the total cleaning costs up to 15% in the “on call” scenario, which corresponds to 1.35 M\$ per year. It is

521 important to point out that this cost reduction is achieved without any additional investment but just taking advantage of
522 the optimized cleaning strategies.

523 The optimization of the cleaning strategies has been applied to two different plant locations with different environmental
524 characteristics in terms of dust concentration and radiative power availability. A sensitivity analysis with regards to
525 airborne dust concentration, electricity price, cleaning speed, and sectorial configuration has finally been performed to
526 prove the strengths of the MILP model and the importance of the cleaning activities in ST plants, giving a remarkable
527 insight of their potential optimization and cost reduction. The results also demonstrate that the economic impact of
528 cleaning is relevant in terms of overall revenues of the plant and hence on the LCOE.

529 Future studies will focus on the refining of the economic model featuring a comparison between different cleaning
530 technologies coupled with a more precise description of the actual O&M cost structure, and on the extension of the
531 optimization algorithm to include the number and the shape of the sectors as variables.

532

533 **Acknowledgements**

534

535 G. Picotti, M.E. Cholette, G. Manzolini, and T. Steinberg acknowledge the support of the Australian Government for this
536 study, through the Australian Renewable Energy Agency (ARENA) within the framework of the Australian Solar Thermal
537 Research Institute (ASTRI – Project ID P52).

538 The authors also acknowledge the Office of Environment and Heritage (OEH) of New South Wales for providing
539 environmental data required for the optimizations.

540

541

542 **References**

543

- 544 Ashley, T., Carrizosa, E., Fernández-Cara, E., 2019. Heliostat field cleaning scheduling for Solar Power Tower
545 plants: A heuristic approach. *Appl. Energy* 235, 653–660.
546 <https://doi.org/10.1016/j.apenergy.2018.11.004>
- 547 Astolfi, M., Binotti, M., Mazzola, S., Zanellato, L., Manzolini, G., 2016. Heliostat aiming point optimization
548 for external tower receiver. *Sol. Energy*. <https://doi.org/10.1016/j.solener.2016.03.042>
- 549 Bergeron, K.D., Freese, J.M., 1981. *Cleaning Strategies for Parabolic-Trough Solar-Collector Fields;*
550 *Guidelines for Decisions*, Sandia National Laboratories.
- 551 Binotti, M., Astolfi, M., Campanari, S., Manzolini, G., Silva, P., 2017. Preliminary assessment of
552 sCO₂ cycles for power generation in CSP solar tower plants. *Appl. Energy* 204.
553 <https://doi.org/10.1016/j.apenergy.2017.05.121>
- 554 Fathi, M., Abderrezek, M., Grana, P., 2017. Technical and economic assessment of cleaning protocol for
555 photovoltaic power plants: Case of Algerian Sahara sites. *Sol. Energy* 147, 358–367.
556 <https://doi.org/10.1016/j.solener.2017.03.053>
- 557 Fernández-García, A., Álvarez-Rodrigo, L., Martínez-Arcos, L., Aguiar, R., Márquez-Payés, J.M., 2014. Study
558 of different cleaning methods for solar reflectors used in CSP plants. *Energy Procedia* 49, 80–89.
559 <https://doi.org/10.1016/j.egypro.2014.03.009>
- 560 Guorobi Optimization, L., 2018. *Gurobi Optimizer Reference Manual* [WWW Document].
- 561 IRENA, IEA-ETSAP, 2013. *Concentrating solar power, Technology Brief*. <https://doi.org/10.1063/1.2993731>
- 562 IRENA Secreteriat, Crespo, L. (ESTELA), Dobrotkova, Z. (IEA), Philibert, C. (IEA), Richter, C. (DLR), Simbolotti,
563 G. (ENEA), Turchi, C. (NREL), Wenhua, X. (UNIDO-I., 2012. *Concentrating Solar Power, Renewable*
564 *Energy Technologies: Cost Analysis Series, Insights*. <https://doi.org/10.1063/1.2993731>
- 565 Jones, R.K., Baras, A., Saeeri, A. Al, Al Qahtani, A., Al Amoudi, A.O., Al Shaya, Y., Alodan, M., Al-Hsaien, S.A.,
566 2016. Optimized Cleaning Cost and Schedule Based on Observed Soiling Conditions for Photovoltaic
567 Plants in Central Saudi Arabia. *IEEE J. Photovoltaics* 6, 730–738.
568 <https://doi.org/10.1109/JPHOTOV.2016.2535308>
- 569 Kutscher, C., Mehos, M., Turchi, C., Glatzmaier, G., Moss, T., 2010. *Line-Focus Solar Power Plant Cost*
570 *Reduction Plan*.
- 571 Larrayoz, A.M., Schöttl, P., Leonardi, E., Les, I., Rohani, S., Pisani, L., 2019. Techno-economic heliostat field
572 optimization: Comparative analysis of different layouts. *Sol. Energy* 180, 601–607.
573 <https://doi.org/10.1016/j.solener.2019.01.053>
- 574 Lofberg, J., 2004. YALMIP : a toolbox for modeling and optimization in MATLAB. 2004 IEEE Int. Conf.
575 *Comput. Aided Control Syst. Des.* 284–289. <https://doi.org/10.1109/CACSD.2004.1393890>
- 576 Manzolini, G., Binotti, M., Bonalumi, D., Invernizzi, C., Iora, P., 2019. CO₂ mixtures as innovative working
577 fluid in power cycles applied to solar plants. Techno-economic assessment. *Sol. Energy* 181, 530–544.
578 <https://doi.org/10.1016/j.solener.2019.01.015>
- 579 Mehos, M., Turchi, C., Vidal, J., Wagner, M., Ma, Z., Ho, C., Kolb, W., Andraka, C., Kruiuzenga, A., 2017.
580 *Concentrating Solar Power Gen3 Demonstration Roadmap*, Nrel/Tp-5500-67464.
581 <https://doi.org/10.2172/1338899>
- 582 NREL, 2017. *Solar pilot* [WWW Document].
- 583 NREL, 2014. *System Advisory Model* [WWW Document].

- 584 Ortigosa, P.M., Redondo, J.L., Berenguel, M., Álvarez, J.D., Cruz, N.C., Salhi, S., 2018. Hector, a new
585 methodology for continuous and pattern-free heliostat field optimization. *Appl. Energy* 225, 1123–
586 1131. <https://doi.org/10.1016/j.apenergy.2018.05.072>
- 587 Pfahl, A., Coventry, J., Röger, M., Wolfertstetter, F., Vásquez-Arango, J.F., Gross, F., Arjomandi, M.,
588 Schwarzbözl, P., Geiger, M., Liedke, P., 2017. Progress in heliostat development. *Sol. Energy* 152, 3–
589 37. <https://doi.org/10.1016/j.solener.2017.03.029>
- 590 Picotti, G., Binotti, M., Cholette, M.E., Borghesani, P., Manzolini, G., Steinberg, T., 2019. Modelling the
591 soiling of heliostats: Assessment of the optical efficiency and impact of cleaning operations. *AIP Conf.*
592 *Proc.* 2126, 30043. <https://doi.org/10.1063/1.5117555>
- 593 Picotti, G., Borghesani, P., Cholette, M.E., Manzolini, G., 2017. Soiling of solar collectors - Modelling
594 approaches for airborne dust and its interactions with surfaces. *Renew. Sustain. Energy Rev.*
595 <https://doi.org/10.1016/j.rser.2017.06.043>
- 596 Picotti, G., Borghesani, P., Manzolini, G., Cholette, M.E., Wang, R., 2018. Development and Experimental
597 Validation of a Physical Model for the Soiling of Mirrors for CSP Industry Applications. *Sol. Energy* 173,
598 1287–1305. <https://doi.org/10.1016/j.solener.2018.08.066>
- 599 Polimeni, S., Binotti, M., Moretti, L., Manzolini, G., 2018. Comparison of sodium and KCl-MgCl_2
600 heat transfer fluids in CSP solar tower with sCO_2 power cycles. *Sol. Energy* 162.
601 <https://doi.org/10.1016/j.solener.2018.01.046>
- 602 Salomé, A., Chhel, F., Flamant, G., Ferrière, A., Thiery, F., 2013. Control of the flux distribution on a solar
603 tower receiver using an optimized aiming point strategy: Application to THEMIS solar tower. *Sol.*
604 *Energy* 94, 352–366. <https://doi.org/10.1016/j.solener.2013.02.025>
- 605 Sánchez-González, A., Santana, D., 2015. Solar flux distribution on central receivers: A projection method
606 from analytic function. *Renew. Energy* 74, 576–587. <https://doi.org/10.1016/j.renene.2014.08.016>
- 607 Sanchez, M., Romero, M., 2006. Methodology for generation of heliostat field layout in central receiver
608 systems based on yearly normalized energy surfaces. *Sol. Energy* 80, 861–874.
- 609 Sarver, T., Al-Qaraghuli, A., Kazmerski, L.L., 2013. A comprehensive review of the impact of dust on the use
610 of solar energy: History, investigations, results, literature, and mitigation approaches. *Renew. Sustain.*
611 *Energy Rev.* 22, 698–733. <https://doi.org/10.1016/j.rser.2012.12.065>
- 612 Seinfeld, J.H., Pandis, S.N., 1998. Atmospheric chemistry and physics: from air pollution to climate change.
613 Wiley-Interscience, New York.
- 614 SolarReserve, n.d. https://issuu.com/solarreserve/docs/solarreserve_crescentdunes-brochure [WWW
615 Document].
- 616 Terhag, F., Wolfertstetter, F., Wilbert, S., Hirsch, T., Schaudt, O., 2019. Optimization of cleaning strategies
617 based on ANN algorithms assessing the benefit of soiling rate forecasts, in: SOLARPACES 2018. p.
618 220005. <https://doi.org/10.1063/1.5117764>
- 619 Truong Ba, H., Cholette, M.E., Wang, R., Borghesani, P., Ma, L., Steinberg, T.A., 2017. Optimal condition-
620 based cleaning of solar power collectors. *Sol. Energy* 157, 762–777.
621 <https://doi.org/10.1016/j.solener.2017.08.076>
- 622 Wang, Z.H., Xu, Z.G., 2018. Optimal Cleaning Schedule of Photovoltaic Module, in: 2018 IEEE IEEM. pp.
623 1637–1641.
- 624 Wolfertstetter, F., Wilbert, S., Dersch, J., Dieckmann, S., Pitz-Paal, R., Ghennioui, A., 2018. Integration of
625 soiling-rate measurements and cleaning strategies in yield analysis of parabolic trough plants. *J. Sol.*
626 *Energy Eng.* 140. <https://doi.org/10.1115/1.4039631>

627

628